Bull Earthquake Eng
DOI 10.1007/s10518-010-9197-3

ORIGINAL RESEARCH PAPER

Probabilistic seismic hazard assessment for Thailand

Teraphan Ornthammarath · Pennung Warnitchai · Kawin Worakanchana · Saeed Zaman · Ragnar Sigbjörnsson · Carlo Giovanni Lai

Received: 22 October 2009 / Accepted: 7 July 2010

Abstract A set of probabilistic seismic hazard maps for Thailand has been derived using procedures developed for the latest US National Seismic Hazard Maps. In contrast to earlier hazard maps for this region, which are mostly computed using seismic source zone delineations, the presented maps are based on the combination of smoothed gridded seismicity, crustal-fault, and subduction source models. Thailand's composite earthquake catalogue is revisited and expanded, covering a study area limited by 0°–30°N Latitude and 88°–110°E Longitude and the instrumental period from 1912 to 2007. The long-term slip rates and estimates of earthquake size from paleoseismological studies are incorporated through a crustal fault source model. Furthermore, the subduction source model is used to model the megathrust Sunda subduction zones, with variable characteristics along the strike of the faults. Epistemic uncertainty is taken into consideration by the logic tree framework incorporating basic quantities, such as different source modelling, maximum cut-off magnitudes and ground motion prediction equations. The ground motion hazard map is presented over a 10 km grid in terms of peak ground acceleration and spectral acceleration at 0.2, 1.0, and 2.0 undamped natural periods and a 5% critical damping ratio for 10 and 2% probabilities of exceedance in 50 years. The presented maps give expected ground motions that are based on more extensive data sources than applied in the development of previous maps. The main findings are that northern and western Thailand are subjected to the highest hazard. The largest contributors to short- and long-period ground motion hazard in the Bangkok region are from the nearby active faults and Sunda subduction zones, respectively.

T. Ornthammarath (✉)
ROSE School, IUSS Pavia, Pavia, Italy
e-mail: tornthammarath@roseschool.it; teraphan@hi.is

T. Ornthammarath · R. Sigbjörnsson
Earthquake Engineering Research Centre, University of Iceland, Selfoss, Iceland

P. Warnitchai · K. Worakanchana · S. Zaman
Asian Institute of Technology, Pathumthani, Thailand

C. G. Lai
European Centre for Training and Research in Earthquake Engineering (EUCENTRE), Pavia, Italy

Published online: 03 August 2010

Keywords Seismic Hazard Map · Thailand · Bangkok

1 Introduction

Thailand is located in the stable Sunda Plate, which has been described as a low and sparse seismicity area. However, after constant improvement of national seismographic stations, a number of frequent small- and medium-sized earthquakes have been revealed, mostly in Northern Thailand, in contrast to general belief. Moreover, since 1975 there have been a number of low- to moderate-sized (M_w 4.5–5.9) shallow-depth earthquake events of Modified Mercalli Intensities (MMI) ranging from VI to VII, causing slight to moderate damage to buildings. Apart from these earthquakes inside Thailand, the boundaries of the Indian and Australian tectonic plates and the Sunda and Burma tectonic plate are considered as zones of high seismicity, with the largest instrumentally recorded event being M_S 7.8 in 1946 (Gutenberg and Richter 1954). The historical record of earthquake damage in Thailand, which dates back to 1545 A.D. earthquake (MMI VIII) in the northern part of the country (Nutalaya et al. 1985), may have been the result of large magnitude and long-distance earthquakes or large magnitude generated along the crustal faults inside Thailand. The ongoing seismic activity alerts the general public as well as the authorities to update national probabilistic seismic hazard maps and eventually the country's seismic design code.

The existing seismic hazard maps in this region (see, e.g., Warnitchai and Lisantono 1996; Shedlock et al. 2000; Pailoplee et al. 2008) have mostly been designed by different author's seismic source zone delineations. These hazard maps were obtained following the classical Cornell (1968) and McGuire (1978) by assuming a uniform rate of seismicity throughout each separated source zone. The intrinsic drawback of this method is that the seismic hazard assessment results can be significantly affected by the delineation of these zones, which could be heavily dependent on the subjective judgment of the hazard analyst. In order to move away from this traditional approach, the smoothed gridded seismicity approach (Frankel 1995) has been successfully adopted in many countries (Frankel 1995; Lapajne et al. 1997, 2003; Garcia et al. 2008). The possible drawback of this method is its strong dependence on quality of the earthquake catalogue (e.g. the positions and sizes of past events) and the smoothing parameters. In a region where historical fault surface ruptures are absent, and the causative seismic sources are largely unknown smoothed gridded seismicity represents the hazard through an earthquake catalogue. For some tectonic structures associated with enough geological and paleoseismic evidence to constrain source locations, crustal fault and subduction source models have been applied. It has also been widely accepted that historical seismicity alone does not satisfactorily reflect the earthquake hazard at low probabilities of exceedance (e.g., 0.0004/year corresponding to 2,475 years return periods).

In this study, new probabilistic seismic hazard maps for Thailand are presented, applying the Frankel (1995) approach with crustal fault and subduction zone models. The compilation of a comprehensive earthquake catalogue for the study region, subsequent processing of catalogue data and selection of appropriate ground-motion prediction equations (GMPEs) are discussed here. Epistemic uncertainty in hazard definition has been tackled within a logic-tree framework. The outcome of the PSHA consists of seismic hazard contour maps for the geometric-mean horizontal component peak ground acceleration (PGA) and spectral accelerations for different natural periods (0.2, 1.0 and 2.0 s) at 5% critical damping ratio,

for reference return periods of 475 and 2,475 years (or 10 and 2% probabilities of exceedance in 50 years, respectively). Only stiff site (760 m/sec average shear wave velocity in the upper 30 m) and level ground conditions are considered here. The seismic hazard computations have been carried out within the national boundary at a grid of 0.1°, approximately 10 km.

2 Thailand and its surrounding tectonic settings

Thailand is situated in the South East Asia (SEA) region, which is located on the boundary of the Indo-Australian and Eurasian plates (Fig. 1). The Indo-Australian and Eurasian boundary zone comprise the convergent margins, including the Burma oblique subduction zone, Andaman thrust and Sunda arc, to the north west, west and south, respectively. Deformation rates across these plate boundaries are variable. The observed seismicity and seismotectonic settings of these plate boundaries clearly indicate the capability of producing large events. A convergence rate of 65–70 mm/year as a result of Australia moving toward SEA is reported by McCaffrey (1996). As India drove into the southern margin of Eurasia, Indochina was rotated clockwise about 25° and extruded to the southeast by approximately 800 km along the Red river and Three Pagoda fault zones during the first 20–30 million years of the collision. The present tectonic stress regime in Thailand is one of transtension, with opening along north-south oriented basins and right-lateral and left-lateral slip on northwest- and northeast-striking faults, respectively (Polachan et al. 1991; Packham 1993).

At the regional scale, the distribution of active deformation in Myanmar is partitioned between the right-lateral Sagaing Fault slipping at 18 mm/year and the Burma subduction zone accommodating 20 mm/year of oblique convergence oriented N30° (Socquet et al. 2006). The Sagaing fault is a major fault running from north to south in Myanmar and believed to be responsible for several earthquakes with magnitudes greater than 7 that occurred in the last century.

An extensive effort in Thailand to document and characterize potentially active faults (Kosuwan et al. 1999, 2000) has been made by the Department of Mineral Resources (DMR), with cooperative research studies by Chulalongkorn University, Thailand, and Akita University, Japan, that evolved from earlier compilations (Hinthong 1995). Fenton et al. (2003) perform paleoseismic investigation in Northern and Western Thailand and identified a number of active faults. These faults are characterized by low slip rates, long recurrence intervals (i.e. thousands to tens of thousands of years), and large magnitude paleoearthquakes (i.e. up to moment magnitude 7). Geomorphic indicators of active faulting of six major faults in Northern Thailand show the sense of slip along these faults as predominantly normal dip-slip. Western Thailand is dissected by a number of northwest- and north-northwest-striking, right-lateral strike-slip faults related to the Sagaing Fault in Myanmar. Although showing much less activity than faults in neighbouring Myanmar, these faults display abundant evidence for late Quaternary movement, including shutter ridges, sag ponds, and laterally offset streams. For Southern Thailand, the Ranong fault extends from the Gulf of Thailand coast southwest toward the Andaman Sea. A few hot springs were found near and along the southern end of the fault, implying that the fault provides significant conduits for the geothermal field. Hot springs in Myanmar and Vietnam are always spatially associated with several active faults.

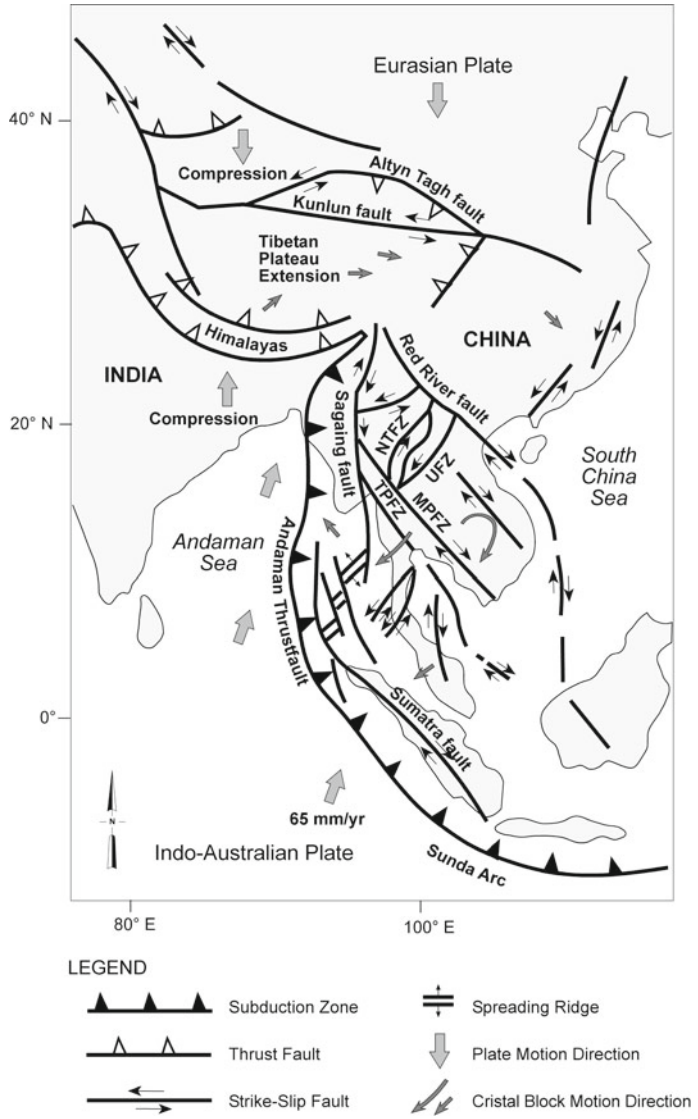

Fig. 1 Major tectonic elements in Southeast Asia and Southern China. *Arrows* show relative directions of motion of crustal blocks during the Late Cenozoic. MPFZ—Mae Ping Fault Zone; NTFZ—Northern Thailand Fault Zone; TPFZ—Three Pagodas Fault Zone; UFZ—Uttaradit Fault Zone. (Courtesy Fenton et al. 2003)

3 Earthquake catalogue

The first historical earthquake recorded in a written document in Thailand was dated back to 624 B.C. (Nutalaya et al. 1985); nevertheless, neither pre-instrumental tremor locations nor their sizes are well constrained. This information is therefore deemed qualitative and not suitable for direct use in quantitative hazard analysis. The instrumental earthquake catalogue for Thailand and neighbouring countries was originally developed under a 4-year research

Table 1 Sample data from the final updated earthquake catalogue

YR	MO	DA	HR	MN	SEC	Lat °	Long °	DEPTH (KM)	MS, mb, ML	Definiton	Mw	Source
1996	8	09	00	26	45.0	12.23	93.64	33	5.70	M_L	5.70	TMD
1996	8	09	23	24	47.0	22.60	98.00	33	4.00	M_L	4.00	TMD
1996	8	10	22	43	37.0	24.71	95.30	33	4.20	m_b	4.60	PDE
1996	8	11	11	04	26.6	14.07	93.73	33	4.00	m_b	4.43	PDE
1996	8	11	11	48	27.9	14.09	93.82	33	4.20	m_b	4.60	PDE
1996	8	11	18	48	12.4	4.26	95.62	100	3.80	m_b	4.26	PDE
1996	8	13	10	33	35.0	22.50	102.00	33	4.20	M_L	4.20	TMD
1996	8	14	16	18	51.0	21.40	99.70	33	3.20	M_L	3.20	TMD
1996	8	16	23	39	38.4	24.42	94.98	33	4.10	m_b	4.52	PDE
1996	8	17	16	41	33.0	21.80	99.20	33	3.30	M_L	3.30	TMD
1996	8	20	08	30	10.9	24.12	94.99	120	4.40	M_S	5.02	PDE
1996	8	23	05	40	41.0	14.71	95.75	33	5.70	M_L	5.70	TMD
1996	8	23	18	53	07.8	21.63	99.25	33	3.30	M_L	3.30	TMD
1996	8	24	03	54	44.0	0.86	99.46	110	5.00	m_b	5.28	PDE

Remarks: *TMD* Thai Meteorological Department
PDE National Earthquake Information Center, USGS)
ISC International Seismological Centre

project, with data compilation and interpretation by the Southeast Asia Association of Seismology and Earthquake Engineering (Nutalaya et al. 1985). The study area was bounded by latitudes 5°–25°N and longitudes 90°–110°E, encompassing Thailand, Indochina, Myanmar, and the southern part of China. Instrumental data were collected from several sources, which include the US Geological Survey (USGS), the US National Oceanic and Atmospheric Administration (NOAA), the International Seismological Centre (ISC), and the Thai Meteorological Department (TMD).

Under a research project entitled "Assessment and Mitigation of Earthquake Risk in Thailand (Phase I)" sponsored by the Thailand Research Fund, this original earthquake catalogue was updated and extended by a research team from TMD. The extended catalogue contains instrumental earthquake records from 1912 to 2002 within a region bounded by latitudes 0°–30°N and longitudes 88°–110°E. In this study, the catalogue was further extended by adding instrumental data recorded by TMD during the period 2003–2007 and the USGS/NEIC Preliminary Determination of Epicenters on-line catalogue (http://neic.usgs.gov). The data of earthquakes from 1977 to 2007 from on-line USGS scientific data (http://earthquake.usgs.gov/research/topic) are also added to the catalogue. The original source of these data is the Global Centroid Moment Tensor catalogue, and the earthquake magnitude is reported using moment magnitude scale. Hence, the final updated catalogue covers earthquakes from 1912 to 2007 in an area covering latitudes 0°N–30°N and longitudes 88°E–110°E. Sample data from the final updated earthquake catalogue are shown in Table 1.

3.1 Magnitude conversion

In the final updated earthquake catalogue, several different magnitude scales are used to define the earthquake magnitude. For example, the 20-s surface-wave magnitude (M_s) and

Table 2 Magnitude conversion relations used in the study

Magnitude	Magnitude range	Magnitude convection relation	Reference
M_s	$3.0 \leq M_s < 6.2$	$M_w = 0.67\, M_s + 2.07\ (\sigma = 0.17)$	Scordilis (2006)
	$6.2 \leq M_s \leq 8.2$	$M_w = 0.99\, M_s + 0.08\ (\sigma = 0.20)$	Scordilis (2006)
m_b	$3.5 \leq m_b \leq 5.5$	$M_w = 0.85\, m_b + 1.03\ (\sigma = 0.29)$	Scordilis (2006)
	$5.5 < m_b \leq 7.3$	$M_w = 1.46\, m_b - 2.42$	Sipkin (2003)
M_L	$M_L \leq 6$	$M_w = M_L$	Heaton et al. (1986)

the short-period P-wave magnitude (m_b) are commonly used in the data from USGS, ISC, and other international database sources, while the local magnitude (M_L) is reported by TMD, and the moment magnitude (M_W) is reported in the Global Centroid Moment Tensor catalogue. It is necessary to convert all these different magnitude scales into a single magnitude scale. In this study, the moment magnitude scale is chosen as the single representative scale. Since the accuracy of reported magnitudes is dependent on magnitude definitions, the more reliable magnitude is then preferred for using in magnitude conversion as follows: M_w, M_s, m_b, and M_L. In this study the local magnitude reported by TMD had been calibrated by comparing it with M_w, and the equation of Heaton et al. (1986) was found to be appropriated. Conversions between magnitude scales are made using the formulae given in Table 2.

After the magnitude conversion, we merged duplicate entries (from different data sources) into a single entry for each earthquake event. The catalogue of unduplicated events contains 14,746 earthquake events with moment magnitudes larger than 3.0.

3.2 Declustering

One basic assumption of the adopted seismic hazard assessment methodology is that earthquake occurrences are statistically independent (the Poisson assumption). Therefore, the earthquake catalogue to be used for seismic hazard assessment must be free of dependent events, such as foreshocks and aftershocks. The process to eliminate dependent events from earthquake catalogues is called "declustering".

Gardner and Knopoff (1974) declustering algorithm, is chosen for the present study. This approach states that foreshocks and aftershocks are dependent (a non-Poissonian process) on the size of the main event, and these earthquake events need to be removed in accordance with space- and time- windows. Normally, a large main earthquake event leads to larger aftershocks over a larger area and for a longer time. Therefore the time- and distance-window parameters for larger main events are greater than those for smaller events. Declustering eliminates about 65% of the events in the catalogue. The final declustered catalogue includes 5,146 earthquake events with M_W greater than or equal to 3.0 in the study region from 1912 to 2007. These earthquake data are plotted in Fig. 2.

3.3 Catalogue completeness

It is recognised that earthquake data in the catalogue are not complete, and that failure to correct for the data incompleteness may lead to underestimation of the mean rates of earthquake occurrence. The correction can be made by identifying the time period of complete data for

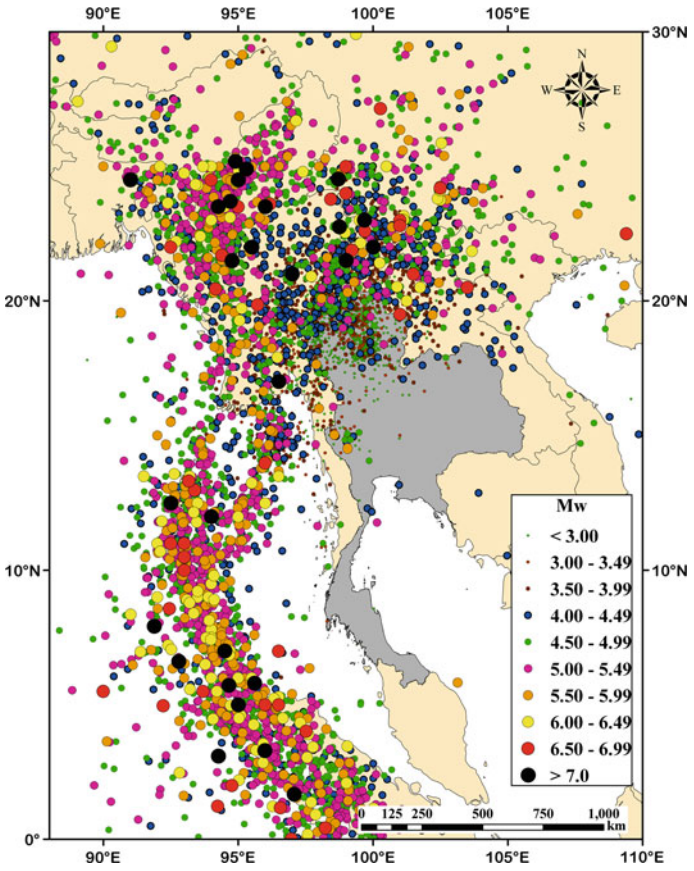

Fig. 2 Thailand and its surrounding seismicity from 1912 to 2007

prescribed earthquake magnitude ranges. Reliable mean rates of earthquake occurrence for the given magnitude ranges can then be computed from the complete data.

Two methods were employed for completeness analysis of the catalogue: (a) the Visual Cumulative method (CUVI) (Tinti and Mulargia 1985) and (b) Stepp's method (Stepp 1973). Both algorithms provided a similar result; hence, the former technique was adopted. We divide the study region into five zones: the three subduction zones (SD-A, SD-B, SD-C) and the two background seismicity zones, i.e., Thailand and its surrounding zone (BG-I), and the remaining zone (BG-II). These five zones are shown in Fig. 3. The data completeness analysis is carried out separately for each of these zones, and the results are presented in Table 3.

4 Modelling of earthquake sources

To properly describe the complex earthquake environments in the region, they are modelled as a mixture of background seismicity, subduction area sources, and crustal faults. These are described in more detail below.

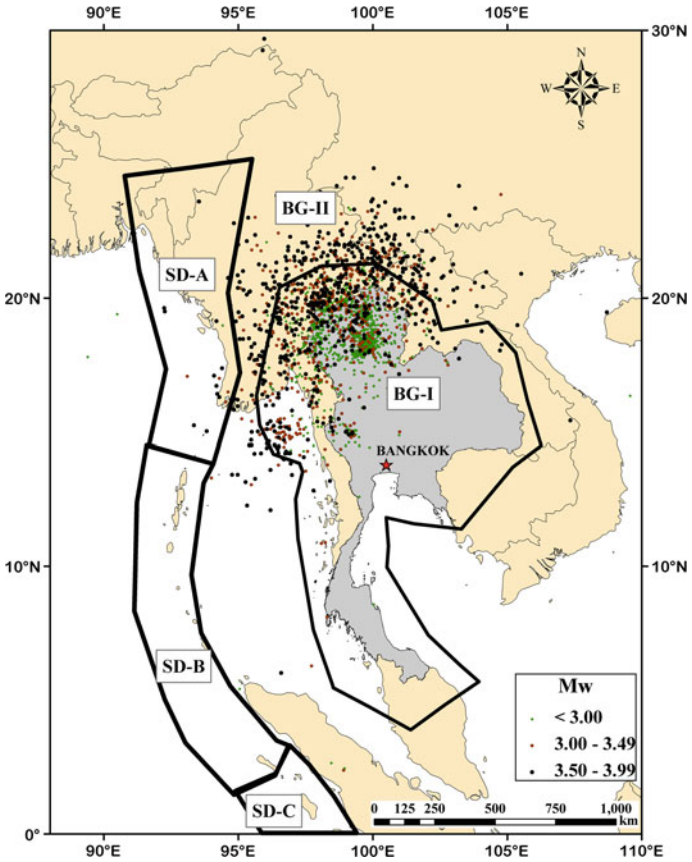

Fig. 3 Background seismicity zones (BG-I and BG-II) and subduction zones (SD-A, SD-B, and SD-C)

Table 3 Time periods of complete data and source parameters

Zone	Magnitude range	a	b	Completeness intervals				
				Mw ≥ 5.00	Mw ≥ 5.50	Mw ≥ 6.00	Mw ≥ 6.50	Mw ≥ 7.00
1 Background seismicity								
BG-I	4.50–6.50	Smooth seismicity	0.90	≥1972	≥1964	≥1930	≥1912	≥1912
BG-II	4.50–7.50		0.90	≥1972	≥1964	≥1930	≥1912	≥1912
2 Subduction source zone								
SD-A	6.50–8.10	5.85	1.02	≥1964	≥1962	≥1955	≥1925	≥1912
SD-B	6.50–9.20	5.49	0.95	≥1960	≥1950	≥1930	≥1925	≥1912
SD-C	6.50–9.20	5.52	1.08	≥1960	≥1950	≥1930	≥1925	≥1912

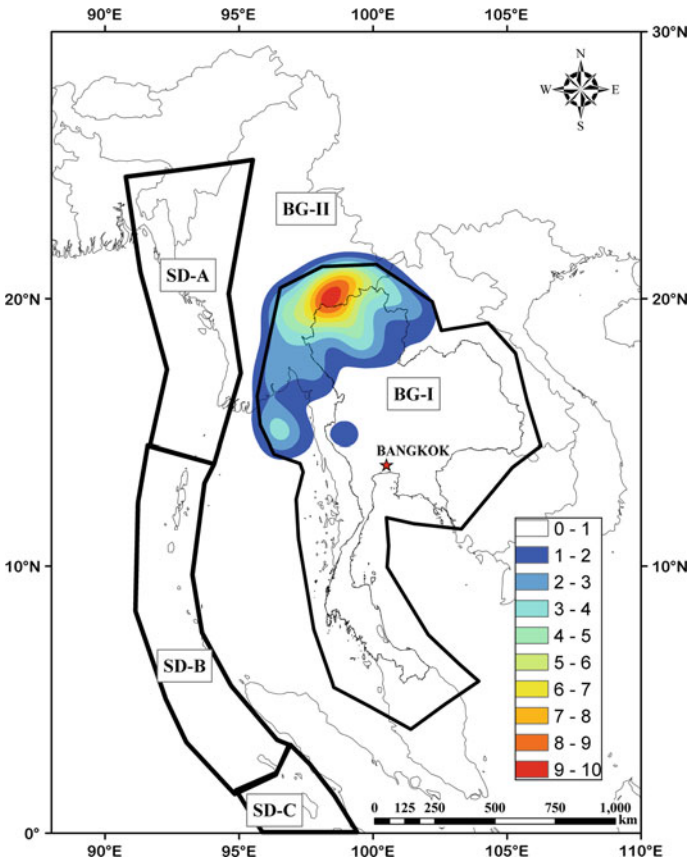

Fig. 4 The smoothed activity rate 10^a value inside BG-I

4.1 Background seismicity model

The background seismicity model represents random earthquakes in the whole study region except the subduction zones. The model accounts for all earthquakes in areas with no mapped seismic faults and for smaller earthquakes in areas with mapped faults. In this approach, it is not necessary to divide the region into many small areas. One large area may be used, but the rate of seismicity is assumed (or allowed) to vary from place-to-place within the area. The rate of seismicity is determined by first overlaying a grid with a given spacing, in the current case 0.10° in latitude and 0.10° in longitude, approximately 10 by 10 km, onto the study region, and counting the number of earthquakes with magnitude greater than a reference value (M_{ref}) in each grid cell. The rate of seismicity is computed by dividing the number of earthquakes by the time period of earthquake data. The rate is then smoothed spatially by a Gaussian-function moving average and comparing with the observed seismicity. By this approach, the spatially-varied seismicity can be modelled with confidence relating to source uncertainty.

In hazard calculations, earthquakes smaller than magnitude 6.0 are characterized as point sources at the centre of each grid cell, whereas earthquakes larger than magnitude 6.0 are assumed to be hypothetical finite vertical or dipping faults centred on the source grid cell.

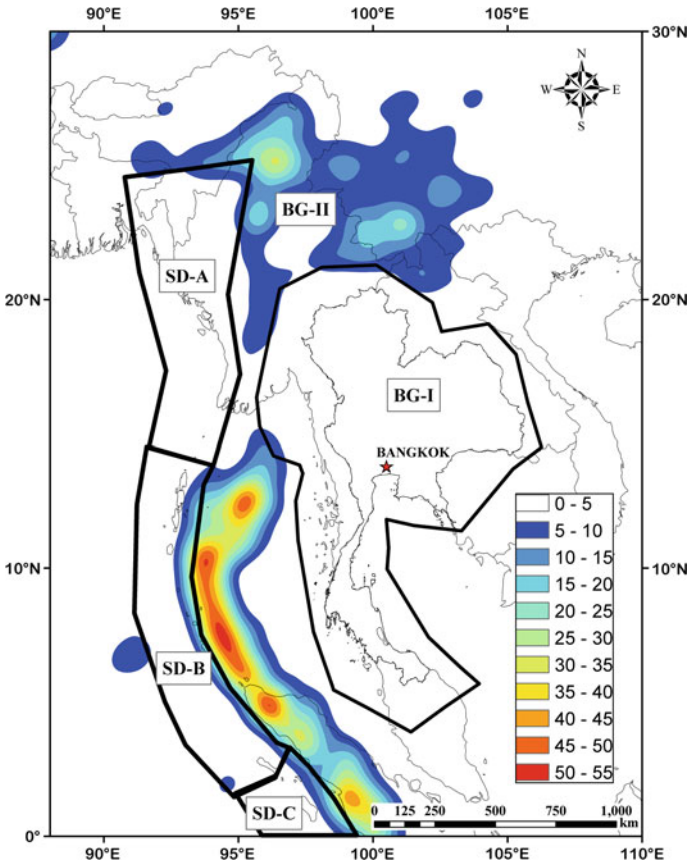

Fig. 5 The smoothed activity rate 10^a value inside BG-II

Lengths of finite faults are determined using the Well and Coppersmith (1994) relations. Consecutively, the precalculated average source-to-site distance from virtual faults with strike directions uniformly distributed is employed (Petersen et al. 2008).

The whole study region is divided into five source zones: BG-I, BG-II, SD-A, SD-B, and SD-C (see Fig. 3). The zones SD-A, SD-B, and SD-C are subduction zones, which will be described in detail below. The zone BG-I is a background seismicity zone covering Thailand and surrounding areas, and the zone BG-II is another background seismicity zone, covering the areas outside Thailand except the three subduction zones.

Earthquake data, particularly small earthquakes, in BG-I are much more completely recorded than those in BG-II. This is due to the high earthquake detection capability of a fairly dense seismograph network in Thailand. Hence, the accuracy of the estimated seismicity rate in BG-I can be significantly improved by including small earthquakes ($3.0 < M_W < 5.0$) in the seismicity rate calculation. Furthermore, this activity rate computation is also based on the observation that moderate earthquakes generally occur in areas where there have been a significant number of magnitude 3 events, (Frankel 1995). On the other hand, in BG-II only earthquake data with $M_W > 5.0$ can be used for computing the seismicity rate due to the incompleteness of small earthquake data. Nevertheless, a lack of small earthquake data is not

a major problem because the seismicity rate in this zone is relatively high; thus, the rate can be reliably estimated from moderate-sized earthquakes. In addition, the overall influence of BG-II on the seismic hazard in Thailand is lower than that of BG-I.

We model the magnitude-dependent characteristic of the seismicity rate in each background seismicity zone by a truncated exponential model (Gutenberg-Richter model):

$$\mathrm{Log}_{10}\left(N(M_W)\right) = a - b\,M_W \tag{1}$$

where $N(M_W)$ is the annual occurrence rate of earthquakes with magnitude greater than or equal to M_W, and a and b are the Gutenberg-Richter model parameters. b is assumed to be uniform throughout the whole background region. Hence, we used complete earthquake data with magnitude greater than 4.0 in both BG-I and BG-II to compute a single regional b-value. The obtained regional b-value is 0.90, and this value is used for both BG-I and BG-II.

The a-value varies from place to place within each zone. It is computed by using a grid with spacing of 0.10° in latitude and longitude and is spatially smoothed using a two-dimensional Gaussian moving average operator with a correlation distance parameter C (Frankel 1995). Earthquake data with $M_W > 3.0$ and $C = 50$ km are used for BG-I, while earthquake data with $M_W > 5.0$ and $C = 75$ km are used for BG-II. The correlation distance is chosen based on Frankel (1995) and it is comparable to earthquake location error. Note that at present there are no fixed rules or guidelines to determine an appropriate C value. If the value of C is too small, the resulting smoothed seismicity will be concentrated around the epicenters of past recorded earthquakes. On the other hand, if the value of C is too large, the resulting smooth seismicity will be blurred and will not reflect the true spatial variation pattern of seismicity. The chosen C values are believed to suitable as the computed smoothed rate 10^a values (presented in Figs. 4, 5) are in agreement to observed spatial pattern of seismicity in Figs. 2 and 3.

In the truncated Gutenberg-Richter models of both BG-I and BG-II, the minimum earthquake magnitude is set equal to 4.5 because earthquakes with smaller magnitude than this are judged not to cause damage to buildings and structures (Bommer et al. 2001). The maximum (upper bound) magnitude is set to 7.5 for BG-II to account for many large earthquakes that have been observed in this zone, as shown in Fig. 2. On the other hand, in BG-I, large earthquakes are already taken into accounted in causative fault modelling and it is unlikely such a great magnitude will go beyond these causative faults (details are shown in the crustal faults section below), so the maximum magnitude for BG-I is set to 6.5.

4.2 Subduction zone model

As explained earlier, the megathrust Sunda subduction zone is divided into 3 sub-zones based on seismicity characteristics: the Burma zone (SD-A), the Northern Sumatra-Andaman zone (SD-B), and the Southern Sumatra zone (SD-C). Each sub-zone is modelled as a seismic area source with a uniform rate of seismicity (the traditional area source model), and the magnitude-dependent seismicity rate is modelled by a truncated Gutenberg-Richter relation.

The calculated Gutenberg-Richter model parameters (a and b values) are shown in Table 3. The minimum earthquake magnitude in the Gutenberg-Richter model is set to 6.5 as the subduction zones are very far from Thailand and hence smaller earthquakes are not important for Thailand. The maximum magnitude for zone SD-A is set to 8.1, which is equal to the maximum observed magnitude plus 0.5 magnitude units. The maximum magnitude for zone SD-B and SD-C is set to 9.2 as the 2004 Sumatra earthquake and the 2005 Nias earthquake

Table 4 Crustal fault source model parameters

No.	Name	Rupture length (km)	Dip angle	Width (km)	Characteristic magnitude	Slip rate (cm/year)			Logic tree weight			Recurrence interval (year)		
						Min	Mean	Max	Min	Mean	Max	Min	Mean	Max
1	*Mae Chan fault*	118	90	15	7.5	0.03	0.07	0.3	0.3	0.4	0.3	11,826	5,068	1,182
2	*Phayao fault*													
	Whole	28	60	17.32	6.8	0.005	0.01	0.1	0.3	0.4	0.3	22,879	11,439	1,144
	Central	13	60	17.32	6.4	0.005	0.01	0.1	0.3	0.4	0.3	13,578	6,789	679
3	*Mae Kuang fault*	35.14	90	15	6.9	–	0.043	–	–	1	–	–	3,367	–
4	*Pua fault*													
	Thung Chang	38.09	60	17.32	6.9	0.01	0.06	0.2	0.3	0.4	0.3	14,077	2,346	704
	Pua	24.68	60	17.32	6.7	0.01	0.06	0.2	0.3	0.4	0.3	10,162	1,694	508
	Santi Suk	12.65	60	17.32	6.4	0.01	0.06	0.2	0.3	0.4	0.3	6,565	1,094	328
5	*Thoen fault*													
	Ban Mai	35	60	17.3	6.88	0.01	0.06	0.2	0.3	0.4	0.3	14,884	2,481	744
	Doi Ton Ngun	25	60	17.3	6.72	0.01	0.06	0.2	0.3	0.4	0.3	11,991	1,998	600
	Mae Than	40	60	17.3	6.94	0.01	0.06	0.2	0.3	0.4	0.3	16,585	2,764	829
6	*Long fault*													
	Northern	31	60	17.32	6.8	0.005	0.01	0.2	0.3	0.4	0.3	24,491	12,245	612
	Southern	20.41	60	17.32	6.6	0.005	0.01	0.2	0.3	0.4	0.3	18,010	9,005	450
7	*Phrae fault*													
	Northern	17.5	60	17.32	6.6	0.005	0.01	0.1	0.3	0.4	0.3	16,494	8,247	825
	Central	26	60	17.32	6.7	0.005	0.01	0.1	0.3	0.4	0.3	21,399	10,699	1,070
	Southern	15	60	17.32	6.5	0.005	0.01	0.1	0.3	0.4	0.3	14,597	7,299	730
8	*Phrae Basin fault*													
	Northern	10	60	17.32	6.3	0.005	0.01	0.1	0.3	0.4	0.3	11,360	5,680	568
	Central	26	60	17.32	6.7	0.005	0.01	0.1	0.3	0.4	0.3	21,399	10,699	1,070

Table 4 continued

No.	Name	Rupture length (km)	Dip angle	Width (km)	Characteristic magnitude	Slip rate (cm/year)			Logic tree weight			Recurrence interval (year)		
						Min	Mean	Max	Min	Mean	Max	Min	Mean	Max
	Southern	15	60	17.32	6.5	0.005	0.01	0.1	0.3	0.4	0.3	14,597	7,299	730
9	*Nam Pat fault*													
	Northern	20	60	17.32	6.6	0.005	0.01	0.1	0.3	0.4	0.3	17,755	8,878	888
	Southern	15	60	17.32	6.5	0.005	0.01	0.1	0.3	0.4	0.3	14,597	7,299	730
10	*Moei fault*	226	90	15	7.5	–	0.036	–	–	1	–	–	5,450	–
11	*Sri Sawat fault*	180	90	15	7.5	0.01	0.05	0.2	0.3	0.4	0.3	24,633	4,927	1,232
12	*Chao Phaya Basin fault*	70	60	17.32	7.3	0.005	0.01	0.1	0.3	0.5	0.2	54,987	27,494	2,749
13	*Three Pagoda fault*													
	Northern	165	90	15	7.5	0.01	0.2	0.4	0.2	0.6	0.2	26,872	1,344	672
	Central	30	90	15	6.8	0.01	0.05	0.2	0.2	0.6	0.2	13,172	2,634	659
	South-West	16	90	15	6.5	0.01	0.05	0.2	0.2	0.6	0.2	8,763	1,753	438
	Sout-East	30	90	15	6.8	0.01	0.05	0.2	0.2	0.6	0.2	13,172	2,634	659
14	*Bong Ti fault*	38.47	90	15	6.9	0.01	0.05	0.2	0.3	0.4	0.3	15,480	3,096	774
15	*Tavoy fault*	120	90	15	7.5	0.1	0.4	1	0.3	0.6	0.1	3,695	924	369
16	*Kungyaungale fault*	55	90	15	7	0.01	0.2	0.4	0.3	0.4	0.3	14,336	717	358
17	*Tenasserim fault*													
	Northern	80	90	15	7.2	0.01	0.2	0.4	0.3	0.4	0.3	19,665	983	492
	Central	100	90	15	7.3	0.01	0.2	0.4	0.3	0.4	0.3	22,222	1,111	556
	Southern	55	90	15	7	0.01	0.2	0.4	0.3	0.4	0.3	14,336	717	358
18	*Ranong fault*													
	Northern	200	90	15	7.6	0.001	0.01	0.05	0.3	0.5	0.2	313,154	31,315	6,263
	Southern	130	90	15	7.4	0.001	0.01	0.05	0.3	0.5	0.2	241,459	24,146	4,829
19	*Chumphon Basin fault*	20	60	17.32	6.6	0.0001	0.001	0.01	0.3	0.4	0.3	857,632	85,763	8,576

Table 4 continued

No.	Name	Rupture length (km)	Dip angle	Width (km)	Characteristic magnitude	Slip rate (cm/year)			Logic tree weight			Recurrence interval (year)		
						Min	Mean	Max	Min	Mean	Max	Min	Mean	Max
20	*Khlong Marui fault*	140	90	15	7.5	0.0001	0.001	0.01	0.3	0.4	0.3	3,167,083	316,708	31,671
21	*Sagaing fault*													
	Northern	346	90	15	7.9	–	1.8	–	–	1	–	–	283	–
	Central	563	90	15	7.9	–	1.8	–	–	1	–	–	174	–
	Southern	482	90	15	7.9	–	1.8	–	–	1	–	–	203	–

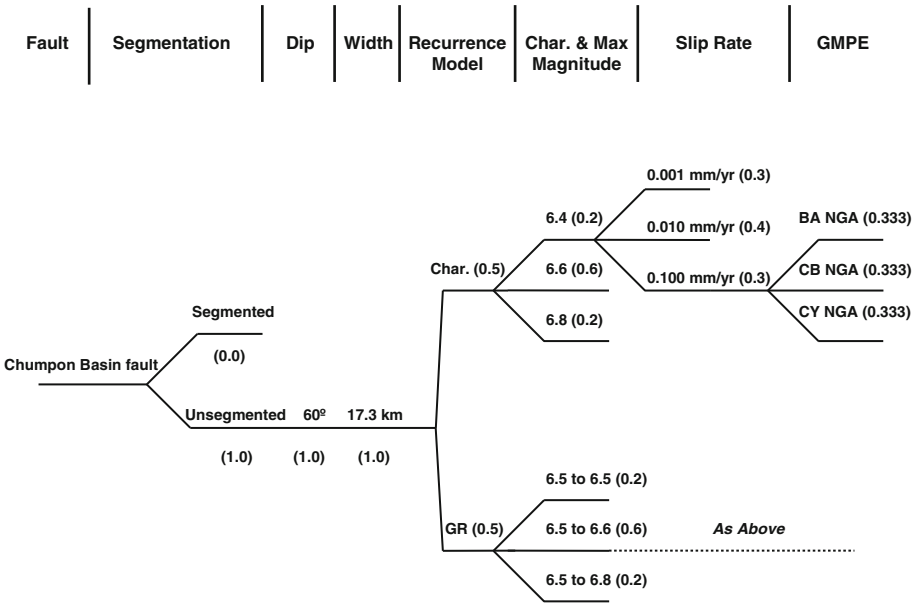

Fig. 6 The Logic Tree for Chumpon Basin fault source model in this study

have already demonstrated the capability of the zones to generate large megathrust earthquakes. A subduction earthquake in each zone is assumed to be created by rupture along an inclined plane at the interface between two tectonic plates. The fault plane ranges from 5 km depth at the left-hand-side zone boundary down to 50 km depth at the right-hand-side zone boundary (Engdahl et al. 2007).

4.3 Crustal fault source model

The information about crustal faults in and near Thailand is mainly obtained from recent paleoseismic investigations carried out by Woodward-Clyde Federal Services in Northern Thailand (DMR 1996), Western Thailand (EGAT 1998) and Southern Thailand (RID 2005). The investigations were conducted using a mix of remote sensing imagery, aerial photographic interpretation and field investigation. The investigation concentrated on the geomorphic expression of faulting, and the comparison of these features with those observed along other active faults around the world. Their important properties and parameters are shown in Table 4 and as an example illustrated by a logic tree diagram in Fig. 6. Twenty-one active seismic crustal faults are modelled explicitly in this study as indicated in Fig. 7. The Sagaing Fault in Myanmar is a major right-lateral strike-slip fault in the study region. The only available assigned slip rate of 18 mm/year is based on high rates of strain accumulation suggested by GPS studies (Socquet et al. 2006 and Petersen et al. 2007). The occurrence rate of large magnitude earthquakes on crustal faults is determined from long-term slip rates and the characteristic earthquake magnitude (M_C). M_C is estimated from expected rupture length, which may be limited by fault segmentation, by using the relation proposed by Wells and Coppersmith (1994).

Two different approaches are employed to model the magnitude-dependent characteristic of the seismicity rate of these crustal faults: the Gutenberg-Richter model and characteristic

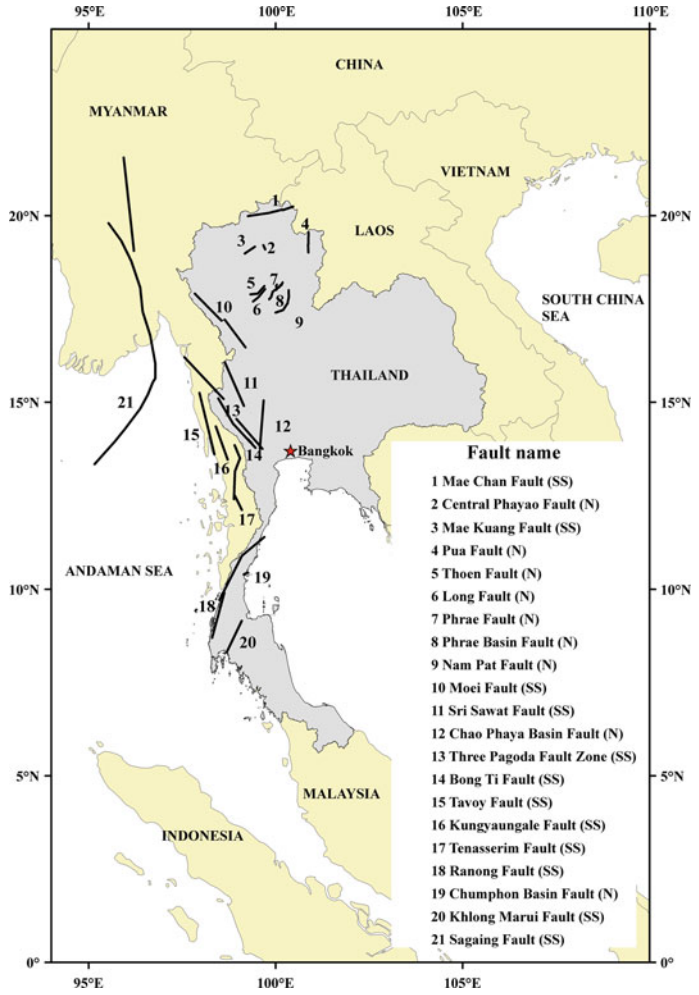

Fig. 7 Twenty-one crustal fault source models incorporating in this study (SS: Strike-Slip fault, N: Normal fault)

earthquake (CE) model. In the Gutenberg-Richter model, a magnitude-frequency distribution for crustal fault model is assumed from the minimum magnitude of 6.5 to the upper-bound magnitude ($M_{\max}$). To account for the uncertainty in estimating $M_{\max}$, we consider three different cases with $M_{\max}$ set equal to $M_C - 0.2$, M_C, and $M_C + 0.2$. The probabilistic weights of 0.2, 0.6, and 0.2 are assigned to these cases, respectively. In each case, the b-value is set equal to the regional b-value of 0.90, and the a-value is determined from the seismic moment rate, which is computed from the fault slip rate (Anderson 1979).

In the characteristic earthquake model, three characteristic earthquake magnitudes are also considered: $M_C - 0.2$, M_C, and $M_C + 0.2$. The probabilistic weights of 0.2, 0.6, and 0.2 are assigned to these cases, respectively. In each case, the earthquake occurrence rate is computed from the characteristic magnitude and the fault slip rate (to match with the seismic moment rate of the fault). The recurrence interval for the characteristic model is determined from:

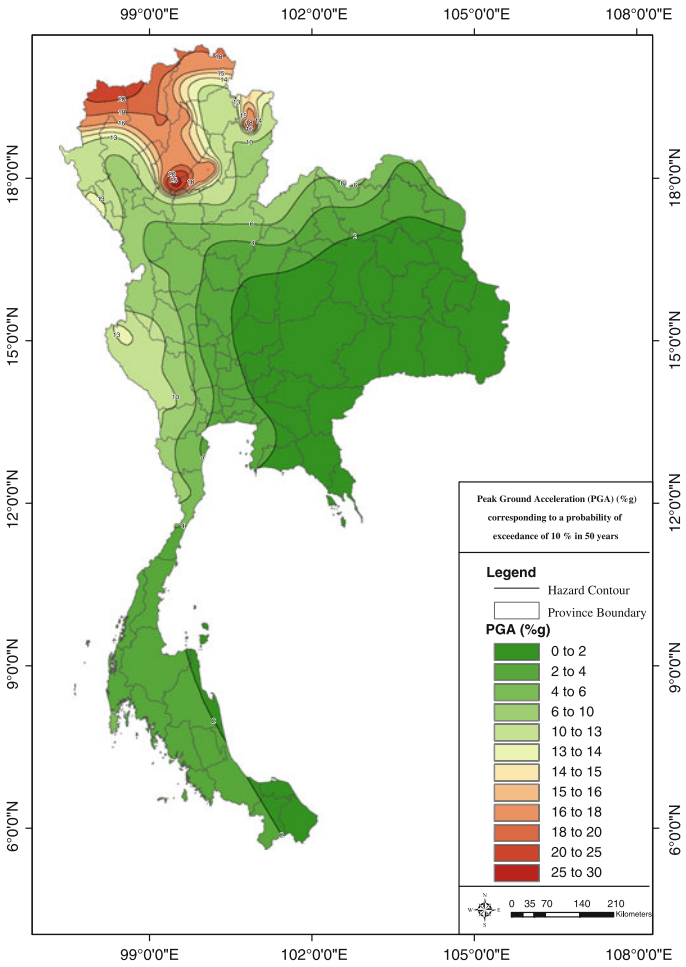

Fig. 8 Thailand hazard maps for PGA corresponding to a probability of exceedance of 10% in 50 years

$$\text{Recurrence Interval} = \mu \dot{u}\, LW / M_{oC} \tag{2}$$

where μ is shear modulus, 3.0×10^{11} dyne/cm^2, L is rupture length, and W is rupture width, $\dot{u}$ is the fault slip rate, M_{oC} is the characteristic earthquake moment, which is calculated from:

$$\log\ (M_{oC}) = 1.5 M_C + 16.05 \tag{3}$$

and the magnitude is assumed to be normally distributed around the characteristic value with a standard deviation of 0.12.

In some areas where the fault location is difficult to constrain or there are several splay faults and its characteristic are better described as a fault zone (i.e. Sri Sawat, Mae Chan, Bong Ti, and the southern part of Sagaing faults), the uncertainty in the location of these faults has been considered in the analysis. Three hypothetical traces fill the space of suspected future earthquake rupture. The central trace, which is either closely located to a lineament from paleoseismic interpretation or approximated from dense seismic activity, is given the highest weight as 0.4, and the other traces are weighted 0.3 each.

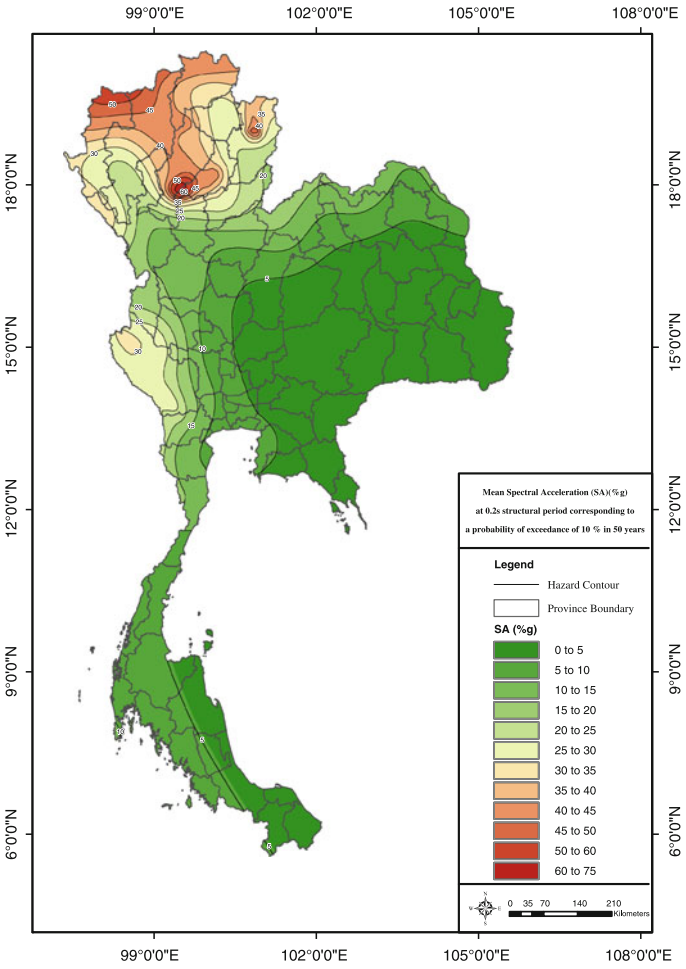

Fig. 9 Thailand hazard maps for spectral accelerations at 0.2s structural period, corresponding to a probability of exceedance of 10% in 50 years

The probabilistic weight in the logic tree for characteristic and Gutenberg-Richter magnitude frequency distributions is assumed equal to 50% each. This has generally increased the expected ground motions compared to the case of considering only the characteristic model. This is because of the more frequent occurrence of earthquakes from Gutenberg-Richter model—particularly those near the lower bound magnitude of 6.5—compared to that of the characteristic model. The characteristic model means that all further ruptures occur along the fault as ruptures of individual segments; nevertheless, historical earthquake ruptures show complex fracture patterns that include significant stop-overs along the full rupture length. Uncertainties are also related to the Gutenberg-Richter model, which predicts more earthquakes smaller than the maximum magnitude than are actually observed. With increasing understanding and enhanced data analysis better constraints on the behaviour of faults in Thailand may eventually emerge. For example, the weighting values could be changed to two-thirds for characteristic earthquakes and one-third for truncated Gutenberg-Richter

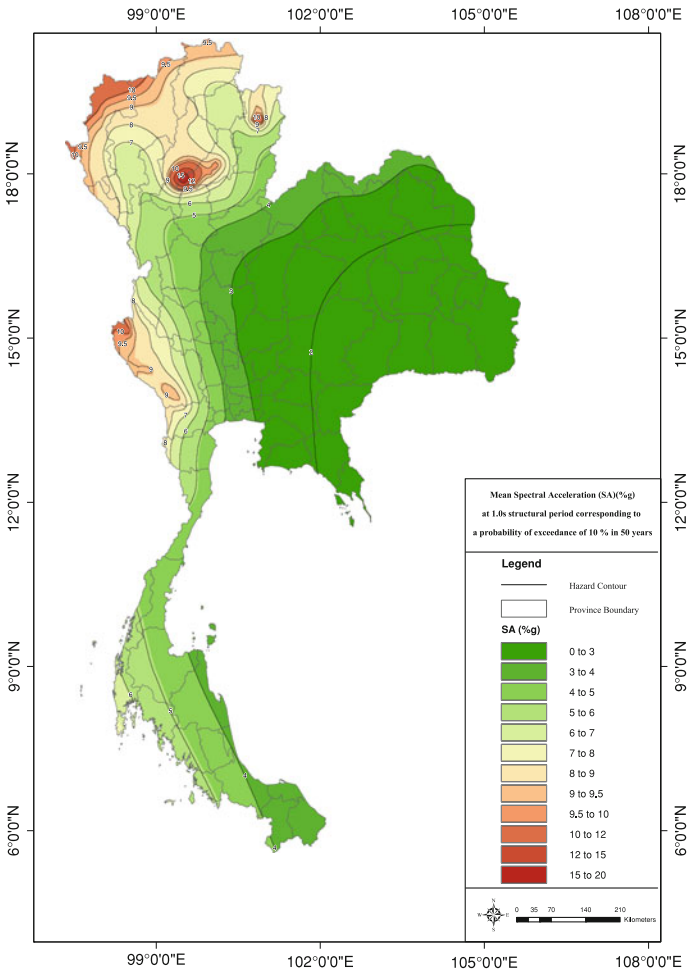

Fig. 10 Thailand hazard maps for spectral accelerations at 1.0s structural period, corresponding to a probability of exceedance of 10% in 50 years

events, as is applied to Californian strike-slip faults (Petersen et al. 2008). The summary of 21 fault parameters is tabulated in Table 4.

5 Ground motion prediction equations

The ground motion parameters, such as PGA, and spectral acceleration (SA), at a given site can be estimated from the earthquake magnitude, source-to-site distance, and local site condition by appropriate Ground motion prediction equations (GMPEs). Traditionally a ground-motion model for a specific region is empirically developed from statistical regression analyses, using available earthquake ground motion records (e.g. Douglas 2003). For the study region, however, a very limited number of strong-motion records are available. One solution to this data limitation is to assume that some existing GMPEs developed for other

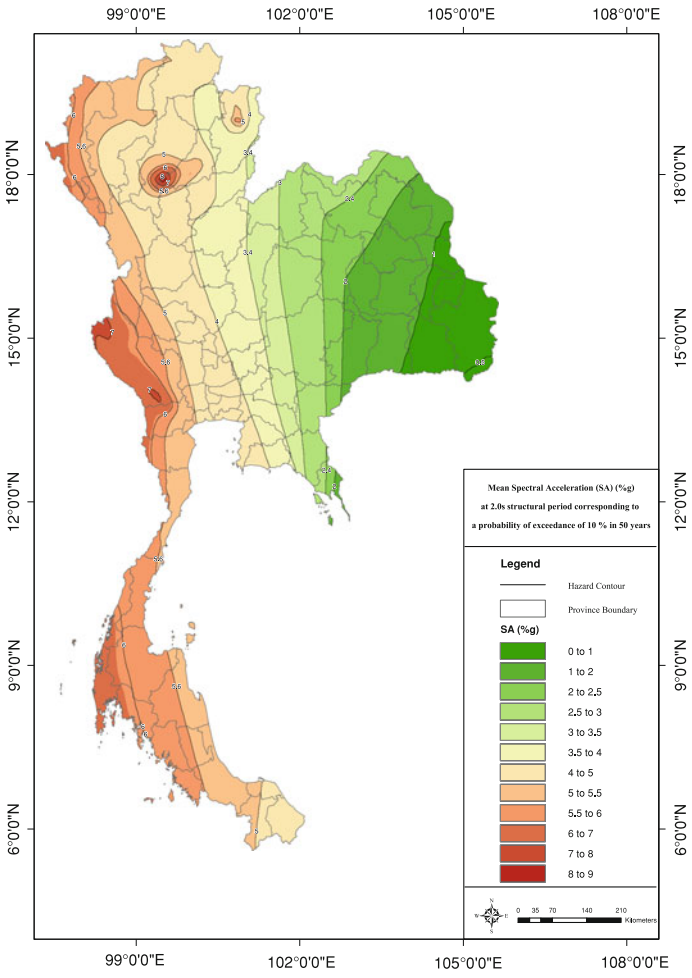

Fig. 11 Thailand hazard maps for spectral accelerations at 2.0s structural period, corresponding to a probability of exceedance of 10% in 50 years

regions with similar seismotectonic characteristics can adequately represent ground-motion scaling in this region.

In this study, three Next Generation Attenuation (NGA) models developed for shallow crustal earthquakes in the western United States and similar active tectonic regions are applied for background earthquakes in BG-I and BG-II and for earthquakes from crustal faults in the study region. These NGA models were developed by Boore and Atkinson (2008), Campbell and Bozorgnia (2008), and Chiou and Youngs (2008) during the NGA project. Sabetta et al. (2005) suggest that the selection of appropriate GMPEs in an analysis has a greater impact than the expert judgement applied in assigning relative weights; therefore, equal probabilities (i.e. 1/3) have been assigned to each of these three models in the logic tree analysis.

For subduction zone earthquakes in SD-A, SD-B and SD-C, we adopt the subduction zone ground-motion models developed by Youngs et al. (1997), Atkinson and Boore (2003, 2008) (both of which are based on global data), and Zhao et al. (2006) (mainly based on Japanese

data). Probabilistic weights assigned to these models are 0.25, 0.25, and 0.50, respectively. The above selected sets of GMPEs as well as their corresponding probabilistic weights are identical to those used by USGS in their recent seismic hazard study of Southeast Asia (Petersen et al. 2007). However, at present, it is not possible to check the validity of these GMPE models in the considered region since there is very little ground-motion data available, but these models are the latest scientific interpretation of ground-motion scaling in their respective regions (Petersen et al. 2007, 2008). The continuing ground-motion monitoring in Thailand will help bring insight to this issue.

6 Probabilistic seismic hazard analysis

The probabilistic seismic hazard analysis (PSHA) is carried out using the USGS software for making and updating the US National Seismic Hazard map (Harmsen 2007). Contour maps have been developed for mean PGA and SA at 0.2, 1.0, and 2.0 s natural periods at 5%

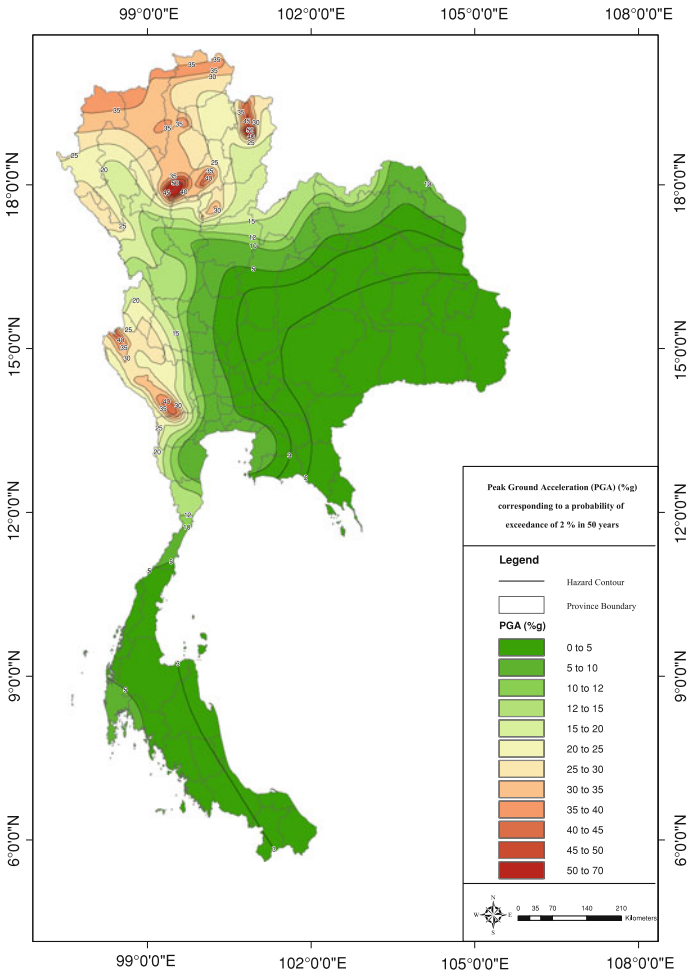

Fig. 12 Thailand hazard maps for PGA corresponding to a probability of exceedance of 2% in 50 years

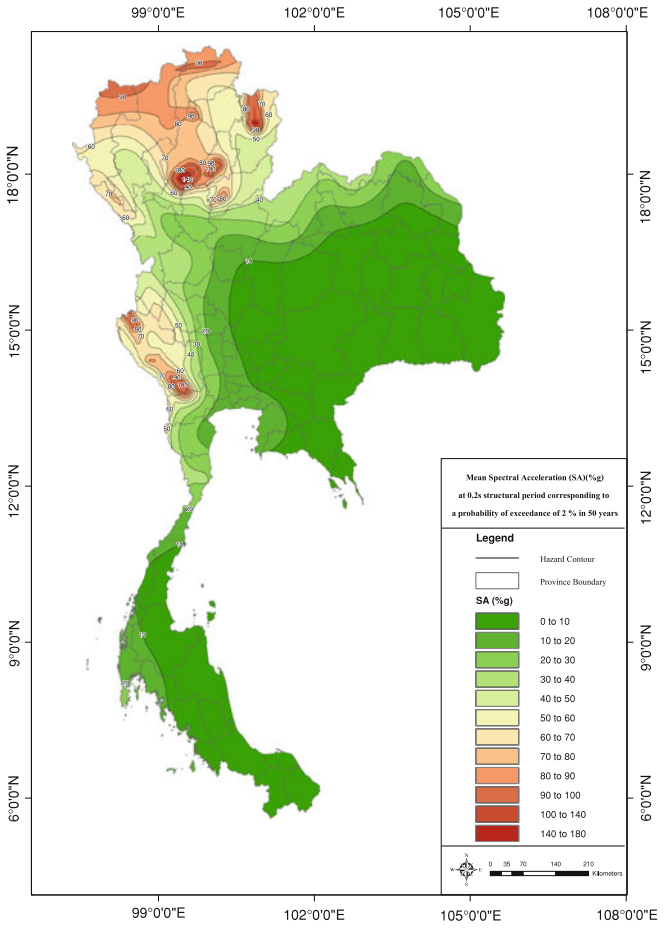

Fig. 13 Thailand hazard maps for spectral accelerations at 0.2s structural period, corresponding to a probability of exceedance of 2% in 50 years

critical damping ratio for 10 and 2% probabilities of exceedance in 50 years, corresponding to 475- and 2,475-year return periods, respectively. The maps are displayed in Figs. 8, 9, 10, 11, 12, 13, 14 and 15. All these seismic hazard maps are based on a reference site condition that is specified to be the boundary between NEHRP classes B and C (rock site), with an average shear-wave velocity in the upper 30 m of the crust of 760 m/s. This is the standard reference site condition for the construction of uniform hazard spectra in many regions (e.g. the USA).

Ground motion across Thailand represented by PGA is in the range of 0.8–28% g, corresponding to the 475-year return period and in the range of 1.3–65% g, corresponding to the 2,475-year return period. For the 475-year return period PGA hazard map, the hazard is fairly well correlated with the seismicity rate 10^a pattern (see Fig. 4). The effect of low-slip-rate crustal faults in Thailand on seismic hazard is not clear on this map. On the other hand, the effect of crustal faults becomes evident in the PGA map (as well as spectral acceleration maps) for the 2,475-year return period. The map clearly shows locally high ground motions at the locations of some major crustal faults. The results confirm the importance of crustal

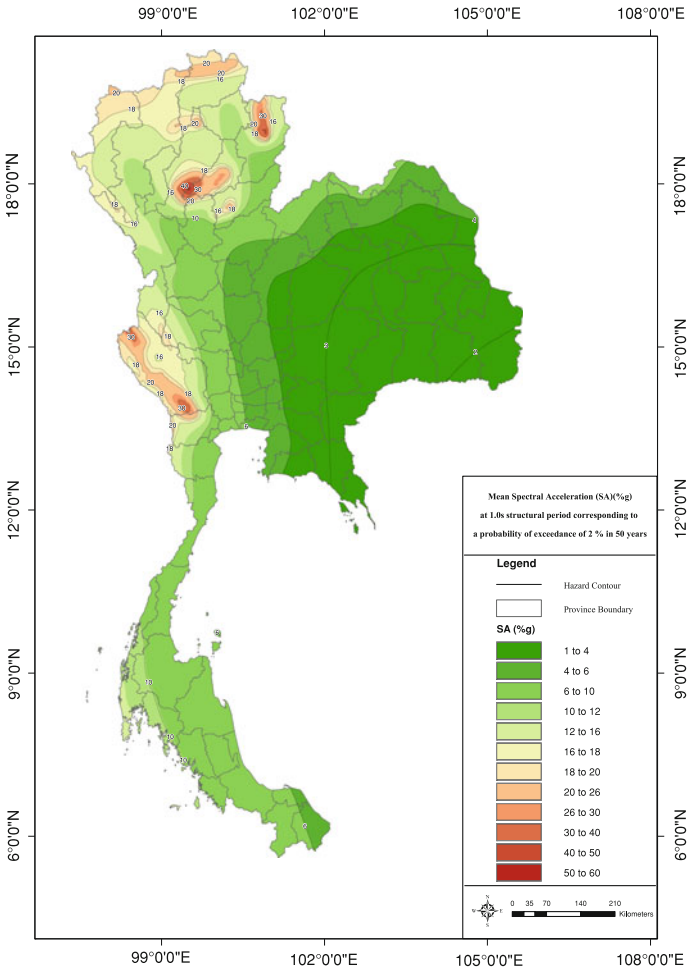

Fig. 14 Thailand hazard maps for spectral accelerations at 1.0s structural period, corresponding to a probability of exceedance of 2% in 50 years

fault sources on the seismic hazard of Thailand. The expected ground motions at the 2% in 50-year level is about a factor of 2.0 higher than the 10% in 50-year values for the Greater Bangkok Area and by a factor in the range of 2.0–3.5 across the highest hazard zone (i.e., northern and western Thailand).

For the long structural periods (1.0 and 2.0 s), most of Thailand is affected by moderate expected ground motions. Because of its long distance from any identified faults and very low recorded seismicity, at least in the last 95 years, most parts of north-eastern Thailand are clearly identified as a low seismic hazard zones. Earthquakes from both near and far sources contribute to the seismic hazard in Bangkok. To gain insight into this issue, hazard curves obtained from the analysis of spectral acceleration at two natural periods are shown in Figs. 16 and 17. Figure 16 represents the hazard curve for stiff structures (0.2 s) at a site in Bangkok, where the main contributor to hazard is nearby crustal faults augmented by relatively infrequent background intraplate events in the stable interior. The 475- and 2,475-year

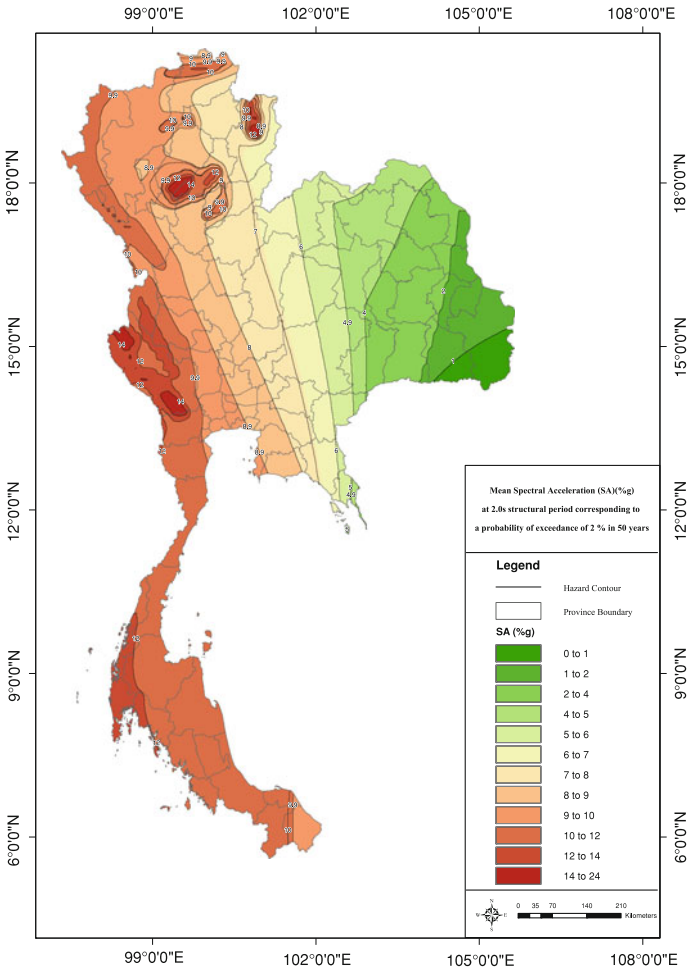

Fig. 15 Thailand hazard maps for spectral accelerations at 2.0s structural period, corresponding to a probability of exceedance of 2% in 50 years

return periods of spectral acceleration at 0.2 s are about 7 and 14.3% g, respectively. The hazard curve for flexible structures (2.0 s), see Fig. 17, is dominated by the Sunda subduction zones, which contributes the largest hazard for both 10 and 2% of exceedance at 50-year levels, 4.5 and 8.9% g, respectively. The noticeable large expected ground motion at 2 s clearly indicates the importance of the subduction zone in defining the seismic design code for Bangkok due to long distance earthquakes (Warnitchai 2004). Of the major cities in Southern Thailand, Phuket has the highest seismic hazard, particularly from the Sunda subduction zones at long structural periods (i.e. T > 1.0 s). The estimated 0.2 s spectral acceleration value of 475- and 2,475-years return periods are 9 and 16.9% g, respectively, and spectral acceleration at 2.0 s of 475- and 2,475-years return periods are 6.5 and 12.5% g, respectively. Overall, by utilizing the combination of seismicity activity and paleoseismic data, the current hazard maps have produced a more explainable expected ground motion than pre-existing maps corresponding to more comprehensive, state-of-the-art models of earthquake sources,

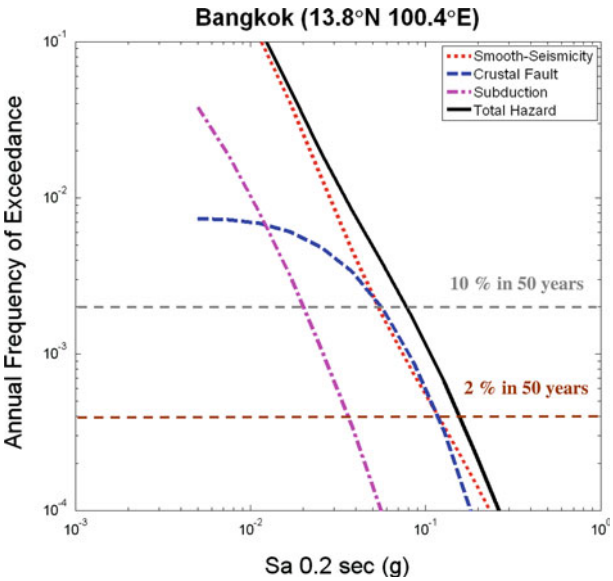

Fig. 16 Computed hazard for spectral acceleration at 0.2 s in Bangkok, and contributions of three different earthquake sources to the hazard

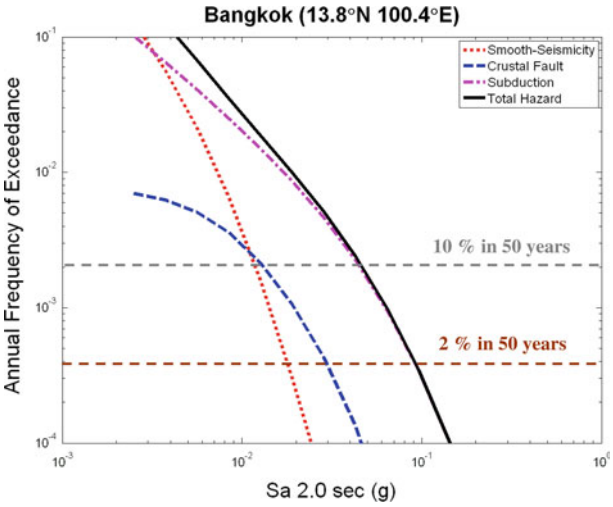

Fig. 17 Computed hazard for spectral acceleration at 2.0 s in Bangkok, and contributions of three different earthquake sources to the hazard

and GMPEs from presently available information while the epistemic uncertainties have also been taking into account through the logic tree approach.

7 Conclusion

The PSHA maps for Thailand has been reassessed and updated by using three models of seismic sources, i.e. spatially smoothed gridded seismicity, crustal-fault, and subduction source models. Two background seismicity models, twenty-one crustal faults, and three subduction zones are assessed from a newly recompiled earthquake catalogue. The characteristic and the Gutenberg-Richter magnitude-frequency models, $M_{\max}$, crustal fault slip rates, three NGA, and three subduction GMPEs have been considered to take epistemic uncertainties into account. The highest hazard areas are located near faults in northern and western Thailand, with the highest PGA exceeding 65% g on stiff soil condition at the 2% in 50-years.

The PSHA has been performed with currently existing data and most recent computerized data interpretation. The authors do recognize that an investigation, based on a meticulous survey of paleoseismological studies, is essential to better constrain source characteristics. Strong ground motion records for earthquakes in this region would be essential to make a more prudent choice of GMPEs. Most of the existing GMPEs have not been developed for the large distances needed to calculate ground motion generated in interplate tectonic environments propagated into intraplate regions. In summary, the hazard maps presented here will certainly change in the future when more information on the aforementioned issues becomes available.

Acknowledgements The authors acknowledge the funding support from Department of Disaster Prevention and Mitigation, Ministry of Interior, Government of Thailand. We wish to thank Stephen Harmsen for providing the code and his suggestions. The authors are much appreciated to many constructive comments from Dr. John Douglas that resulted in several improvements. Special thanks are extended to graduate students, School of Engineering and Technology, AIT, Thailand, for their technical supports in GIS data. The authors are grateful to two anonymous reviewers for constructive comments that enhanced the quality of the paper.

References

Anderson JG (1979) Estimating the seismicity from geological structures for seismic-risk studies. Bull Seism Soc Am 69(1):135–158

Atkinson GM, Boore DM (2003) Empirical ground-motion relations for Subduction-zone earthquakes and their application to Cascadia and other regions. Bull Seism Soc Am 93(4):1703–1729

Atkinson GM, Boore DM (2008) Erratum to empirical ground-motion relations for subduction zone earthquakes and their application to Cascadia and other regions. Bull Seism Soc Am 98(5):2567–2569

Bommer JJ, Georgallides G, Tromans I (2001) Is there a near-field for small-to-moderate magnitude earthquakes?J Earthq Eng 5(3):395–423

Boore DM, Atkinson GM (2008) Ground-motion prediction equations for the average horizontal component of PGA, PGV, and 5%-damped PSA at spectral periods between 0.01 s and 10.0 s. Earthq Spectra 24(1):99–138

Campbell KW, Bozorgnia Y (2008) Ground motion model for the geometric mean horizontal component of PGA, PGV, PGD and 5% damped linear elastic response spectra for periods ranging from 0.01 to 10.0 s. Earthq Spectra 24(1):139–171

Chiou B, Youngs R (2008) A NGA model for the average horizontal component of peak ground motion and response spectra. Earthq Spectra 24(1):173–215

Cornell CA (1968) Engineering seismic risk analysis. Bull Seism Soc Am 58(5):1583–1606

DMR (1996) Department of mineral resources, environmental Impact assessment: geological aspect, Kaeng Sua Ten Dam Project, Changwat Phrae, Main Report No. 3, Ministry of Industry, Thailand

Douglas J (2003) Earthquake ground motion estimation using strong-motion records: a review of equations for the estimation of peak ground acceleration and response spectral ordinates. Earth-Sci Rev 61: 43–104

EGAT (1998) Electricity Generating Authority of Thailand, Preliminary Seismic Hazard Evaluation of Khao Laem and Srinagarind Dams, Thailand

Engdahl RE, Villasenor A, Deshon RH, Thurber CH (2007) Teleseismic relocation and assessment of seismicity (1918–2005) in the region of the 2004 M_W 9.0 Sumatra-Andaman and 2005 M_W 8.6 Nias Island Great Earthquakes. Bull Seism Soc Am 97(1A):S43–S61

Fenton CH, Charusiri P, Wood SH (2003) Recent paleoseismic investigations in northern and western Thailand. Anna Geophys 46:957–981

Frankel A (1995) Mapping seismic hazard in the Central and Eastern United States. Seismol Res Lett 66(4): 8–21

Garcia J, Slejko D, Rebez A, Santulin M, Alvarez L (2008) Seismic hazard map for Cuba and adjacent areas using the spatially smoothed seismicity approach. J Earthq Eng 12(2):173–196

Gardner JK, Knopoff L (1974) Is the sequence of earthquakes in southern California, with aftershocks removed, Poissonian? Bull Seism Soc Am 64(5):1363–1367

Gutenberg B, Richter C (1954) Seismicity of the earth and associated phenomena. Princeton University Press, Princeton

Harmsen S (2007) USGS Software for probabilistic Seismic Hazard Analysis (PSHA) Draft Document. Geological Survey, U.S. (http://earthquake.usgs.gov/research/hazmaps/product_data/2008/software)

Heaton TH, Tajima F, Mori AW (1986) Estimating ground motions using recorded accelerograms. Surv Geophy 8:25–83

Hinthong C (1995) The study of active faults in Thailand. In: Proceedings of the annual technical 1995 conference on the progression and vision of mineral resources development

Kosuwan S, Hinthong C, Charusiri P (1999) The preliminary use of MapInfo programme to earthquake hazard assessment in Thailand and mainland SE Asia. J Geol Ser B 13–14:174–178

Kosuwan S, Hinthong C, Charusiri P (2000) The preliminary use of MapInfo programme to earthquake hazard assessment in Thailand and mainland SE Asia. In: Proceedings of the 12th world conference on earthquake engineering: New Zealand society for earthquake Engineering, Upper Hutt, 12, paper number 0108

Lapajne JK, Motnikar BS, Zabukovec B, Zupancic P (1997) Spatially smoothed seismicity modelling of seismic hazard in Slovenia. J Seismol 1(1):73–85

Lapajne JK, Motnikar BS, Zupancic P (2003) Probabilistic seismic hazard assessment methodology for distributed seismicity. Bull Seism Soc Am 93(6):2502–2515

Le Dain AY, Tapponier P, Molinar P (1984) Active faulting and tectonics of Burma and surrounding regions. J Geophys Res 89:453–472

McCaffrey R (1996) Slip partitioning at convergent plate boundaries of SE Asia. In: Hall R, Blundell DJ (eds) Tectonic evolution of Southeast Asia. Geol Soc Spec Publ 106:3–18

McGuire RK (1978) FRISK: computer program for seismic risk analysis using faults as earthquake sources, U.S. Geological Survey Open-File Report 78-1007

Nutalaya P, Sodsri S, Arnold EP (1985) SEASEE Series on Seismology, vol II—Thailand, Southeast Asia Association of Seismology and Earthquake Engineering and U.S. Geological Survey

Packham GH (1993) Plate tectonics and the development of sedimentary basins of the dextral regime in Western Southeast Asia. J Southeast Asian Earth Sci 8(1–4):497–511

Pailoplee S, Sugiyama Y, Charusiri P (2008) Probabilistic seismic hazard analysis in Thailand and adjacent areas by using regional seismic source zones. In: Proceedings of the international symposia on geoscience resources and environments of Asian terranes (GREAT 2008), 4th IGCP 516, and 5th APSEG; November 24–26, 2008, Bangkok

Petersen MD, Dewey J, Hartzell S, Mueller C, Harmsen S, Frankel AD, Rukstales K (2004) Probabilistic seismic hazard analysis for Sumatra. Indonesia and across the southern Malaysian Peninsula. Tectonophysics 390:141–158

Petersen M, Harmsen S, Mueller C, Haller K, Dewey J, Luco N, Crone A, Lidke D, Rukstales K (2007) Documentation for the Southeast Asia Seismic Hazard Maps, Administrative Report, U.S. Geological Survey, p 65

Petersen M, Frankel AD, Harmsen S, Mueller C, Haller K, Wheeler RL, Wesson RL, Zeng Y, Boyd OS, Perkins DM, Luco N, Field EH, Wills CJ, Rukstales KS (2008) Documentation for the 2008 Update of the United States National Seismic Hazard Maps. Open-File Report 2008-1128 US Geological Survey, p 128

Polachan S, Pradidtan S, Tongtaow C, Janmaha S, Intrawijitr K, Sangsuwan C (1991) Development of Cenozoic basins in Thailand. Mar Pet Geol 8:84–97

RID (2005) Royal Irrigation Department, Seismic Hazard Evaluation of The Tha Sae Project, Thailand, Final Report prepared by URS Corporation

Sabetta F, Lucantoni A, Bungum H, Bommer JJ (2005) Sensitivity of PSHA results to ground motion prediction relations and logic tree weights. Soil Dyn Earthq Eng 25:317–329

Scordilis EM (2006) Empirical global relations converting MS and mb to moment magnitude. J Seismol 10:225–236

Shedlock KM, Giardini D, Grünthal G, Zhang P (2000) The GSHAP global seismic hazard map. Seismol Res Lett 71(6):679–689

Sipkin SA (2003) A correction to body-wave magnitude mb based on moment magnitude M_W. Seismol Res Lett 74(6):739–742

Socquet A, Vigny C, Chamot-Rooke N, Simons W, Rangin C, Ambrosius B (2006) India and Sunda plates motion and deformation along their boundary in Myanmar determined by GPS. J Geophys Res 111:B05406. doi:10.1029/2005JB003877

Stepp JC (1973) Analysis of completeness of the earthquake sample in the Puget Sound area. In: Harding ST (ed) Seismic Zoning. NOAA Tech. Report ERL 267-ESL30, Boulder

Tinti S, Mulargia F (1985) Completeness analysis of a seismic catalog. Anna Geophys 3:407–414

Warnitchai P, Lisantono A (1996) Probabilistic seismic risk mapping for Thailand. In: Proceeding of the 11th world conference on earthquake engineering, Acapulco, June 23–28 paper number 1271

Warnitchai P (2004) Development of seismic design requirements for buildings in Bangkok against the effects of distant large earthquakes. In: Proceedings of the 13th world conference on earthquake Engineering (13WCEE), Vancouver, August 1–6, 2004, paper number 744

Wells DL, Coppersmith KJ (1994) New empirical relationships among magnitude, rupture length, rupture width, and surface displacements. Bull Seism Soc Am 84(4):974–1002

Youngs RR, Chiou SJ, Silva WJ, Humphrey JR (1997) Strong ground motion attenuation relationships for subduction zone earthquakes. Seismol Res Lett 68(1):58–73

Zhao JX, Zhang J, Asano A, Ohno Y, Oouchi T, Takahashi T, Ogawa H, Irikura K, Thio H, Somerville P, Fukushima Y, Fukushima Y (2006) Attenuation relations of strong ground motion in Japan using site classification based on predominant period. Bull Seism Soc Am 96(3):898–913